Chapter 3

Laboratory testing programme

3.1 Introduction

An understanding and quantification of the mechanical properties of the materials constituting the geocell reinforced soil support packs is a prerequisite for the understanding of the functioning of the composite structure. Laboratory tests were performed on the fill material and the plastic membrane material in addition to the tests performed on the composite structures. This chapter presents the results of the laboratory testing programme.

3.2 Tests on the fill material

The fill material was obtained from Savuka Mine's backfilling plant. Savuka mine is part of Anglo Gold's operations near Carletonville. The mine operates mainly on the Ventersdorp Contact Reef and the Carbon Leader Reef of the Witwatersrand Complex.

The tailings material is cycloned in the backfilling plant to reduce the < 40 μm fines contents and is normally referred to as classified tailings. Classified tailings are widely being used in mines as a backfill to provide regional support in mined stopes and is a logical choice for a fill material for support packs.

The laboratory tests performed on the fill material were:

- Basic indicator tests, including particle size distribution, specific gravity, Atterberg limits and minimum and maximum density tests.
- Light- and Scanning Electron Microscope (SEM) imaging were also performed on different particle size ranges.
- Isotropic and triaxial compression as well as oedometer tests.

3.2.1 Basic indicator tests

A grading analyses, Atterberg limits and a specific gravity test were performed commercially by Soillab (Pty) Ltd. on a sample of the fill material.

Specific gravity

This test was performed according to the SABS 844 standard. The Specific gravity obtained for the sample was 2.75 Mg/m^3.

Grading analyses

Wet sieving and hydrometer testing were performed to obtain the grain size distribution of the material. The tests were performed according to the South African standard test method, TMH1 A1 (wet sieving) and TMH1 A6 (hydrometer test), which is equivalent to the ASTM D422-63 test method. Figure 3.1 shows the result of the grading analyses.

Atterberg limits

Even though it would be expected that the parent tailings material will show plastic limits of between 22% and 39% and liquid limits of between 29% and 56% (Vermeulen, 2001) the Atterberg limits are not applicable to the material due to the fact that the cycloning process removes the clay sized particles from the soil resulting in the material being non-plastic.

3.2.2 Material compaction

Compaction tests on the cycloned gold tailings material test were performed according to the South African standard test method, TMH1 A7, which is equivalent to the "Modified AASHTO" method (AASHTO T180-61). The test result is shown in Figure 3.2. The maximum density of the classified tailings is 1620±9 kg/m^3 at a moisture content of about 17.5%. This maximum density corresponds to a minimum voids ratio, e_{min} = 0.68.

The minimum density test was performed according to the British standard test method, BS 1377 Part4:1990:4.3. The repeatability of the test was high and consistent results were obtained. The minimum density for the material is 1234 kg/m^3 which corresponds to a maximum voids ratio, e_{max} = 1.23.

The maximum density was also achieved via a method of vibration compaction. The equipment necessary for the ASTM D4253–93 was not available. The following non-standard test was performed:

As for the minimum density test, a one litre cylinder was filled with 1 kg of oven-dried material. After inverting the cylinder a few times, to loosen the soil, it was turned upside down to accumulate all the soil at the top of the cylinder. At this point the cylinder was quickly turned over and placed on a standard concrete laboratory vibrating table. The volume of the soil was recorded and used to calculate the minimum density of the soil. The vibration table was then switched on and the volume of the soil recorded with the time of vibration. This procedure was repeated several times. The results are presented in Figure 3.3.

The time of vibration is a measure of the compaction energy. It can clearly be seen that the density reaches a maximum value after which no increase in the density takes place with extra compaction energy added. The value of the maximum density obtained from this non-standard test is 1600±12 kg/m^3.

3.2.3 Microscopy on the material grains

Vermeulen (2001) pointed out that although it is convenient to simplify soils as continuum media for analytical purposes, it is the properties at particle level that ultimately control its engineering behaviour.

Information on the particle shape and surface texture was gained by studying the material particles under optical and electron microscopes. A sample of the classified tailings material was separated into 10 size-ranges of which a specimen each was prepared for microscopic analyses (Table 3.1).

The original soil sample was treated with a dispersant solution of Sodium hexametaphosphate and separated into a courser and finer section by washing it through the 63 μm sieve. The > 63 μm portion was wet sieved to separate it into the sizes shown in Table 3.1, while the < 63 μm portion was separated by settlement in water. The following procedure was used to separate the < 63μm portion of the material:

The < 63 μm was mixed with water in a 1000 ml sedimentation cylinder normally used for hydrometer tests. The suspension was thoroughly mixed and placed on the table for the settlement time of 2 minutes after which the remaining suspension was carefully decanted into another sedimentation

cylinder. The material that settled out in the original cylinder was carefully washed out of the cylinder into a bowl. In the bowl the material was mixed and, again, allowed to settle out for 2 minutes. The remaining suspension was carefully decanted and the material dried.

Table 3.1 Nominal grain sizes of specimens separated for microscopy analyses.

No.	Nominal size	Separation method	Description
1	212 μm	>212 μm sieve	medium/fine sand
2	150 μm	>150 μm sieve	Fine sand
3	125 μm	>125 μm sieve	Fine sand
4	75 μm	>75 μm sieve	Fine sand
5	63 μm	>63 μm sieve	Fine sand/Coarse silt
6	30 μm	2 min settlement	Coarse silt
7	20 μm	4 min settlement	Coarse/Medium silt
8	10 μm	15 min settlement	Medium silt
9	6 μm	60 min settlement	Medium/fine silt
10	3 μm	240 min settlement	Fine silt

The suspension that was decanted from the original sedimentation cylinder was mixed and placed on the table for 4 minutes. After completion of the settlement time the remaining suspension was carefully decanted into another sedimentation cylinder, the sedimentation washed into a bowl, mixed and allowed to settle out for 4 minutes. The suspension remaining in the bowl, after the settlement time, was decanted and the material dried. This process was repeated to separate the smaller particles, each time allowing a longer settlement period (Table 3.1).

The dried material was mounted on the microscope stage using conductive double-sided carbon tape. These specimens were then studied under the light microscope. After completion of the study with the light microscope, the specimens were coated with a thin coating of gold to ensure conductivity, which is essential for the Scanning Electron Microscopy (SEM). The gold coating was applied by the sputter method. The coating was applied in five stages, lasting 10 seconds each, to prevent overheating of the specimens. During the imaging process the beam of electrons was accelerated using a voltage of 5 kV.

Images produced by the light and electron microscopy is shown in Figure 3.4 to Figure 3.17

3.2.4 Compression tests on soil

Oedometer tests, isotropic compression tests and drained triaxial compression tests were performed on the classified tailings. Two methods were used to prepare the triaxial test samples. The first method was moist tamping, while the second method was dry compaction.

Moist tamping is a sample preparation technique commonly used for the preparation of silty soil samples. Dry soil material was thoroughly mixed with a small known percentage of water. The specimens were prepared in five separate equal-volume lifts. Care was taken to compact each layer to the desired density by measuring its height during the compaction process. After compaction, the top and bottom surfaces were carefully levelled in order to minimise possible bedding errors occurring during the testing of the sample.

The preparation of samples via the dry compaction method was done as follows: As with the moist tamping, the sample was prepared in five layers. The oven dried soil of each layer was inserted and compacted. After compaction of the dry material of a layer, water was added before commencing with the compaction of the dry material of the next layer. The dry compaction of the soil was the method used in the preparation of the geocell packs. With dry compaction the achievable densities were higher than with moist tamping although a lower compaction effort was used with the dry compaction method.

Extreme care was taken to trim the sample ends to smooth planar surfaces in order to minimize the possible bedding error. Misalignment errors were minimized by using a round nosed loading ram and a flat loading plate.

The oedometer test specimens were prepared dry inside the odometer ring. The loose specimen were prepared by carefully placing dry material inside the ring in a loose state while the dense specimen was prepared by lightly compacting the dry material in the oedometer ring.

The oedometer tests were prepared and performed by the author. The samples for the isotropic consolidation and triaxial compression testing were prepared by the author and the tests were conducted under his supervision.

Oedometer tests

Oedometer tests were performed on two soil samples. These samples were prepared dry. The first test sample was at a medium dense state with a relative

density, D_r, of 44% with an initial voids ratio, e_0, of 0.987. The second test was performed on a dense sample with a D_r of 69% and an e_0 of 0.848. The results of these tests are presented in Figure 3.18.

Isotropic compression tests

The isotropic compression tests were performed according to the guidelines given in BS 1377:1990 Parts 5 and 6. Non-lubricated end platens were used in the isotropic compression tests. One of the samples was a 50 mm diameter sample while the other samples were 75 mm diameter samples.

Volume change in the samples was measured with an external burette type volume change gage. The sample deformation was measured externally with dial gauges while the load on the sample was measured externally with a dial gauge and proving ring. The pore pressure was measured externally with electronic pressure transducers.

A total of ten isotropic compression tests were performed on samples with an initial voids ratio ranging between 0.84 and 0.71 ($D_r \approx 70\% - 95\%$). The mean effective stress at the end of the isotropic compression test ranged from 50 kPa to 250 kPa. Four samples were prepared with the moist tamping method and six samples were prepared dry. Table 3.2 gives a summary of the performed isotropic compression tests.

Table 3.2 Isotropic compression tests performed on the classified tailings material.

B	Sample density (kg/m^3)		e_o	e_a	Mean effective stress, p', at end of test	Sample preparation method
	Before compression	After compression				
0.98	1496	1505	0.839	0.828	125	Moist tamping
0.99	1517	1530	0.813	0.798	250	Moist tamping
0.98	1531	1537	0.797	0.790	100	Moist tamping
0.99	1539	1542	0.787	0.784	75	Dry compaction
0.99	1553	1559	0.771	0.764	100	Moist tamping
0.97	1563	1568	0.760	0.754	75	Dry compaction
1	1566	1569	0.757	0.753	50	Dry compaction
0.99	1581	1587	0.740	0.733	100	Dry compaction
0.96	1592	1600	0.728	0.719	175	Dry compaction
0.98	1605	1614	0.714	0.704	250	Dry compaction

B = Skempton's pore pressure parameter, e_o = voids ratio after compaction, e_a = voids ratio after isotropic compression

The test results of these tests are shown in terms of the voids ratio and mean effective stress in Figure 3.19. These results are plotted together with the results from the oedometer test in Figure 3.20. for this purpose the mean effective stress for the oedometer tests was calculated by assuming Jáky's (1944, 1948) equation for the earth pressure coefficient at rest and assuming the friction angle, $\phi' = 40°$, i.e.:

$$K_0 = 1 - \sin(\phi') \tag{3.1}$$

Where:

K_0 = the coefficient of earth pressure at rest,

ϕ' = the Mohr-Coulomb friction angle.

Triaxial compression tests

After completion of each isotropic consolidation test a drained triaxial compression test were performed on the sample according to the guidelines given in BS 1377:1990 Part 8.

The triaxial samples were strained at 0.1 mm/min. Area and membrane corrections were applied to the test data but no corrections were made for volume change due to membrane penetration. Due to the fineness of the soil the error associated with the membrane penetration was negligible and the magnitude of this error was estimated to be less than 0.02% using the theory presented by Molenkamp and Luger (1981). The test results are shown in Figure 3.21 and Figure 3.22 and summarized in Table 3.3.

Table 3.3 Results of drained triaxial compression tests performed on the classified tailings material.

Initial density (kg/m^3)	Peak stress (kPa)				strain at peak (%)		Sample preparation method
	q'	p'	σ_1'	σ_3'	ε_a	ε_v	
1505	419	266	545	126	6.25	-1.05	Moist tamping
1530	770	504	1020	246	5.80	-0.65	Moist tamping
1537	366	220	464	98	3.77	-1.02	Moist tamping
1542	304	177	380	76	6.77	-1.35	Dry compaction
1559	378	225	477	99	3.85	-1.42	Moist tamping
1568	281	170	357	76	5.98	-1.25	Dry compaction
1569	202	119	254	52	6.28	-0.73	Dry compaction
1587	427	241	526	99	8.72	-2.42	Dry compaction
1600	743	423	918	175	6.39	-1.80	Dry compaction

q' = deviatoric stress, p' = mean effective stress, σ_1' = axial stress, σ_3' = confining stress, ε_a = axial strain, ε_v = volumetric strain

3.3 Tests on membrane material

The Hyson Cell geocells used in this study are manufactured from High Density Polyethylene (HDPE) sheets with a nominal thickness of 0.2 mm. Due to the viscoelastic nature of HDPE the yield stress and stiffness of the membrane at lower strain rates is lower than that obtained at higher strain rates. It is therefore important to investigate the strain-rate-dependence of the membrane stress-strain curves.

Geomembranes are normally tested by one of three methods. The method most often used is the uniaxial tensile test as described in ASTM D638-94. The second is the wide-strip tensile test (ASTM D4885-88). The third test is known as the multiaxial tension test (ASTM D5617-94) which, due to the sophistication of the method and the specialized apparatus needed for the tests, is not used as often as the other two methods.

The difference in the three methods essentially lies in the boundary conditions imposed onto the test specimen. It is important that the chosen tests should as close as possible represent the strain condition expected in the field.

The uniaxial tensile test does not provide lateral restraint to the specimen during testing and essentially tests the geomembrane under uniaxial stress conditions. The wide-strip tensile test is generally considered representative of plane strain loading of the membrane. During the wide-strip tensile test lateral restraint is imposed onto the specimen at the grips while the middle portion of the specimen is not restrained. The wide-strip tensile test provides boundary conditions varying from plane strain conditions at the grips to uniaxial tensile loading in the middle of the specimen (Merry and Bray, 1996). The multiaxial tensile test provides a plane strain boundary condition at the edge of the specimen, which changes to an isotropic biaxial state at the centre (Merry and Bray, 1997).

As the membranes of a geocell cell are stretched in the direction normal to the cell axis and allowed to contract parallel to the cell axis, the membrane deforms essentially under plane stress conditions similar to a membrane in uniaxial loading (Figure 3.23). Uniaxial tests were therefore performed on the membrane material. All tests were performed in the machine direction of the plastic, as the geocells was manufactured with the machine direction of the membranes perpendicular to the geocell cell axis.

A series of uniaxial tensile tests on the membrane material were carried out at strain rates ranging between 50%/min and 0.05%/min. Constant grip separation speed was specified for each test. The tests were performed at 22 ± 1 °C. Table 3.4 provides a summary of the tensile tests performed on the membrane material.

Table 3.4 Summary of uniaxial tensile tests performed on the HDPE membranes.

Cross head speed (mm/min)	Width (mm)	Thickness (mm)	Length between grips (mm)	Initial engineering strain rate (%/min)*	
100	100	0.177	193	51.8	(50)
100	100	0.175	197	50.8	(50)
60	100	0.18	196	30.7	(30)
50	100.5	0.175	197	25.4	(25)
50	100	0.178	196	25.5	(25)
25	100.5	0.18	193	12.9	(12.5)
10	100	0.179	197	5.09	(5)
10	100	0.186	196	5.1	(5)
5	101	0.179	198	2.52	(2.5)
1.25	101	0.183	193	0.647	(0.625)
0.50	100.5	0.191	193	0.259	(0.25)
0.25	99.5	0.189	194	0.129	(0.125)
0.194	100	0.186	197	0.098	(0.1)
0.10	101.5	0.188	195	0.051	(0.05)
0.075	101	0.182	197	0.038	(0.038)

* Nominal strain rate used in this document given in brackets

As the calculation of the stress in the membrane is dependent on the cross-sectional area of the membrane, scatter in the results increases as the width of the specimen decreases. This is due to small variations in the thickness of the specimen. The repeatability of the tests was therefore increased by maximizing the width of the test specimen. The width of the test specimens was fixed at the available clamp width of 100 mm.

The length of the tests specimens (between the grips) was fixed at about 200 mm. Merry and Bray (1996) showed that the stress-strain results of membranes tested in uniaxial tensile tests are not sensitive to the aspect ratio of the test specimen, provided that local strain measurements are used (Figure 3.24). The author assumed that a specimen length of two times the width was long enough to provide an uniaxial stress condition over the central half of the specimen. This assumption appears to be acceptable. Support for this assumption is given in Chapter 4.

Studies on the strain distribution within a membrane in uniaxial testing have shown that a non-uniform distribution of strain can be expected in the membrane making local measurement of strains important (Giroud et al., 1994; Merry and Bray, 1996). This can also be seen in Figure 3.25, showing photographs of the deformed membranes during a uniaxial tensile test.

Local strain measurement devices were, however, not available. The longitudinal strain was calculated from the grip separation and a correction factor applied to obtain the local longitudinal strain. The correction factor was obtained from photographic methods. A Pentax Z-1 camera with a Pentax 100-300 lens was used for this purpose. The lens distortion was tested by photographing graph paper and measuring the distortion on the photographs. For this lens the distortion was negligible and no correction was necessary.

Each plastic membrane was marked before testing and photographs of the membrane, and a reference scale in the plane of the membrane, were taken during the course of the tests. The distance between the marks on the membrane were measured on the photographs and used in calculating the local strain. The local longitudinal strains were calculated over the central quarter of the specimen. The results of the local strain measurements compared to the strain from the grip separation are shown in Figure 3.26.

The method used for measuring the local longitudinal strain was also used to obtain the lateral strain at the centre of the test which is shown in Figure 3.27. The data shown in the figure was obtained from photographs taken during the tests, as well as from direct measurements of the permanent deformation of the membranes after removal of the test specimen from the test machine. From Figure 3.27 it can be seen that the engineering Poisson's ratio for the HDPE membrane reduces throughout the test.

The stress-strain curves for the uniaxial tensile tests on the membranes are presented in Figure 3.28. In Figure 3.28 the membrane stress is calculated by assuming a constant width and thickness. This is the way tensile test results on geomembranes are most often presented and is referred to as engineering stress.

3.4 Tests on geocell-soil composite – single geocell structure

Compression tests on soil-geocell composite structures consisting of single cells were performed. The purpose of these tests were to investigate the fill-membrane interaction in order to facilitate the understanding of the more complex multi-cell composite structure.

Single cells with a nominal width and height of 100 mm and 200 mm were cut from the manufactured geocell honeycomb structure. The resulting tube-like cells were placed on steel plates and filled with the classified tailings material. Flaps of ducting tape was stuck to the bottom periphery of the plastic cells and folded inside to prevent the dry soil from running out at the bottom, when the cells were filled.

The soil was compacted by hand with a steel tamping rod, in layers of 15 - 20mm thick. High densities could be achieved with relatively little compaction effort when the soil was compacted dry.

The soil was compacted inside the plastic geocells. During the compaction process the plastic geocells were not supported. This allowed the membrane to stretch during the compaction process to generate a small initial confining stress.

After compaction the dimensions of the soil-filled geocell were measured. The height was measured at four different positions and the diameters at four positions equally spaced along the periphery at the specimen top, bottom, middle and quarter heights. The diameter at each of the vertical positions was taken as the mean of the measured diameters at that position and the volume of the specimen was calculated with the use of Simpson's integration rule. The dimensions and densities of the tested samples are shown in Table 3.5.

Table 3.5 Geometric data for the single geocell specimens.

Test	D_0 (mm)	L_0 (mm)	Density (kg/m^3)	Strain rate (1/min)
O	102	210	1600*	9.5×10^{-3}
A	98.8	191.5	1593	
B	95.78	192	1601	5.2×10^{-3}
C	88.6	191.37	1605	

D_0 – original diameter, L_0 – original height
* Approximate density

Two sets of tests were performed. The first was instrumented to measure the circumferential strain of the sample. A 0.25 mm steel guitar string was wrapped around the sample once with one end fixed to a stationary point and the other to a Linear Variable Differential Transformer (LVDT) (Figure 3.29). "Beads" were cut from nylon tubes with a 4 mm OD and 2 mm ID. These "beads" were strung onto the steel string to prevent the string from "cutting " into the specimens. The circumferential displacement was measured at quarter heights and at the centre of the specimen. The results of these measurements are shown in Figure 3.30. It was afterwards realized that the resistance of the LVDT's as well as the friction between the strings and the nylon "beads" has caused an unknown, small but non-trivial confining stress on the sample and the strength measurements for this test were discarded.

Equivalent tests on the second set of specimens were subsequently performed without the circumferential strain measured. Figure 3.31 shows test specimen A in the test machine. The results of these tests are shown in Figure 3.32.

For all the tests a stiff loading plate was placed on the specimens, with a steel ball placed between the loading ram and the platen to ensure that the load was applied uniformly to the specimen.

3.5 Tests on geocell-soil composite – multiple geocell structures

Three compression tests on multi-cell geocell-soil composite packs were performed. The tested packs consisted of a square grid of 2x2, 3x3 and 7x7 cells respectively (Figure 3.33). All three packs had a nominal aspect ratio (width/height) of 0.5. Table 3.6 summarises the geometries of the tested packs.

Table 3.6 Geometric data for the tested multi-cell specimens.

test	W_c (mm)	W_0 (mm)	L_0 (mm)	Area (m^2)	Density (kg/m^3)	Strain rate (1/min)
2x2	98 (110)	220	402	0.044	1567	$5x10^{-3}$
3x3	75 (85)	250	442	0.058	1550	$3.3x10^{-3}$
7x7	73 (83)	525	995	0.275	1576	$2x10^{-3}$

W_c – mean cell width (diameter for circular cells given in brackets),
W_0 – original nominal pack width, L_0 – original pack height;

The multi-cell specimens were prepared with the same procedure described in Section 3.4 for the single cell composite structures. The fill was compacted in lifts of 50 – 75 mm and as a result the density that was achieved was less than that obtained for the single cell specimens.

Photographs were taken of the top surface of the pack before testing which enabled the digitising of the cross sectional geometries and the calculation of the cross sectional area. The volume of the packs were estimated using direct measurements of the pack cross sectional geometry and the height as well as the digitised top area.

As with the single cell specimens, the soil was compacted inside the unsupported plastic geocell structures. The inner membranes of the composite structure formed straight boundaries between the inner cells while the outer membranes bulged to form a bubble shaped structure (Figure 3.34).

A small amount of stretching of the membranes took place during the compaction process.

The packs were cut from the commercially manufactured plastic honeycomb structure. The lenient manufacturing tolerance resulted in a variation in the cell sizes visible in Figure 3.34.

The packs were instrumented with several LVDT's as shown in Figure 3.35. The 2x2 pack was instrumented with two LVDT's at the mid-height of the pack. Four LVDT's were placed externally and three were placed "internally" for the 3x3 and 7x7 cell packs. The three "internal" LVDT's were placed outside the pack and linked to a telescopic tube system fixed to the inner membranes. The "internal" LVDT system is illustrated in Figure 3.36. Sharp edged tubes equivalent to the tubes used in the telescopic system were used to cut circular holes in the plastic membranes through which the telescopic system was placed. The telescopic tubes were fixed to the plastic by sandwiching the membrane between two nuts and washers. The nuts and washers also served to reinforce the hole in the plastic membrane. The hole in the outside membrane was reinforced with a 15mm square piece of ducting tape fixed to the plastic before cutting the hole.

The "internal" LVDT's were placed at the mid-height of the packs and allowed to move with the pack. The external LVDT's were fixed at the original placement height and a systematic measurement error occurred due to the axial shortening of the packs. Assuming the pack sides to deform in a parabolic

shape, the measured data can be corrected for the systematic error by applying the following correction factor for which the derivation is given in Appendix A:

$$f = \frac{1}{1-\left(\frac{\varepsilon_a}{1-\varepsilon_a}\right)^2} \tag{3.2}$$

Where:

f = the correction factor for the measured deformation,

ε_a = the axial strain

This systematic error is estimated to vary between 0% at the start of the test to 6% at an axial strain of 20%.

Figures 3.37 to 3.40 show the results of the compression tests on the multi-cell packs. Because of the different cell sizes the measured displacements are given in terms of engineering strain, rather than displacement, in order to facilitate comparison.

Figure 3.37 shows the stress strain response of the 2x2 cell, the 3x3 cell and the 7x7 cell pack. Figure 3.38 presents the results for the 2x2 cell pack. The results from the two external LVDT's are presented in Figure 3.38(b).

Figure 3.39 presents the results for the 3x3 cell pack. The results from the "internal" LVDT's and "external" LVDT's are presented in Figure 3.39(b) and (c) respectively. In Figure 3.39(b) the mean strain for the outer cells is shown along with the measured strain for the cells C1, C2 and C3. This was calculated from the sum of the deformation of C1 and C3 divided by the sum of the original cell widths. Along with the results from the measurements of the outer LVDT's in Figure 3.39(c), the total strain over the width of the pack (series O4), is also shown. This was calculated from the sum of the deformation of the cells C1, C2 and C3.

The variation of the cell sizes has caused a geometric eccentricity in the pack which resulted in the pack yielding in a buckling mode after the peak stress had been reached. The buckling took place in the direction, away from the LVDT's 1, 2 and 3 shown in Figure 3.35(a). This can be seen from the sudden change in the slope of the lines calculated from the measurements of the outer LVDT's (Figure 3.39(c)). The horizontal strain at the mid height of the pack is therefore better presented by series O4, which will be used for comparison purposes.

The strain value from series O4 closely follows the values of O1, O2 and O3 up to the peak strain. The data show that the buckling deformation mode only developed after the peak stress had been reached.

Figure 3.40 shows the results of the 7x7 cell pack. The results obtained from the "internal" LVDT's are shown in Figure 3.40(b). Series C4 in this figure represents the strain of the centre cell and was calculated from the deformation of cells C1, C2 and C3 as well as the deformation of the outer membrane measured with the external LVDT. The results obtained from the outer LVDT's are shown in Figure 3.40(c)

Figures 3.41 and 3.42 show the deformed geometry of the 3x3 and 7x7 packs after completion of the compression tests. The stroke of the tests machine allowed for about 20% axial strain on the 7x7 cell pack. After completion of the compression test on the 7x7 cell packs, the test machine was retracted and, spacers placed between the pack and the loading platen and the compression test continued.

After completion of the compression tests the cells were carefully cut open and removed as shown in Figure 3.43 and Figure 3.44 enabling the internal deformed geometry to be studied. It was possible to distinguish the "dead zone" in the pack as a result of the permanent deformation of the plastic membranes. Measurements of the depth of the "dead zone" in the pack were made. It should be mentioned that the location of the boundary of the "dead zone" was subject to some degree of subjective interpretation. Due to the symmetry about the $x = 0$, the $y = 0$ and the $x = y$ axes, measurements at symmetrically equivalent locations were treated as separate data points at the same location. The mean, minimum and maximum values measured at each symmetrically equivalent location are shown in Figure 3.45.

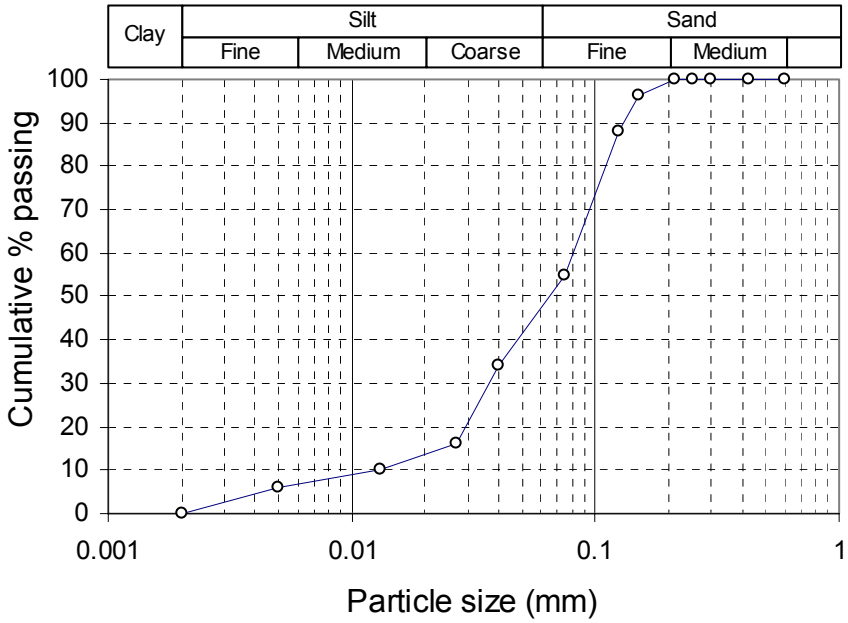

Figure 3.1 Particle size distribution of the classified tailings.

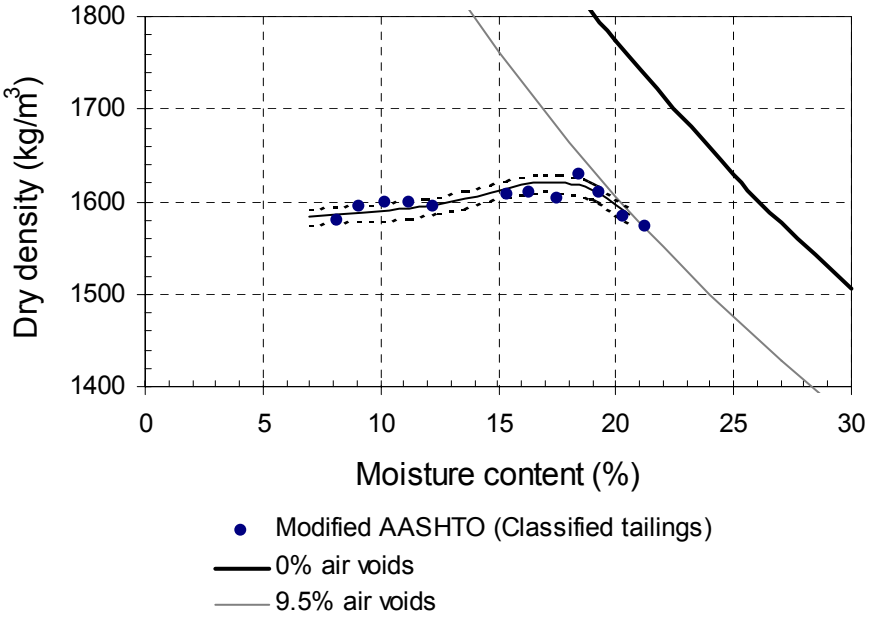

Figure 3.2 Results of compaction tests.

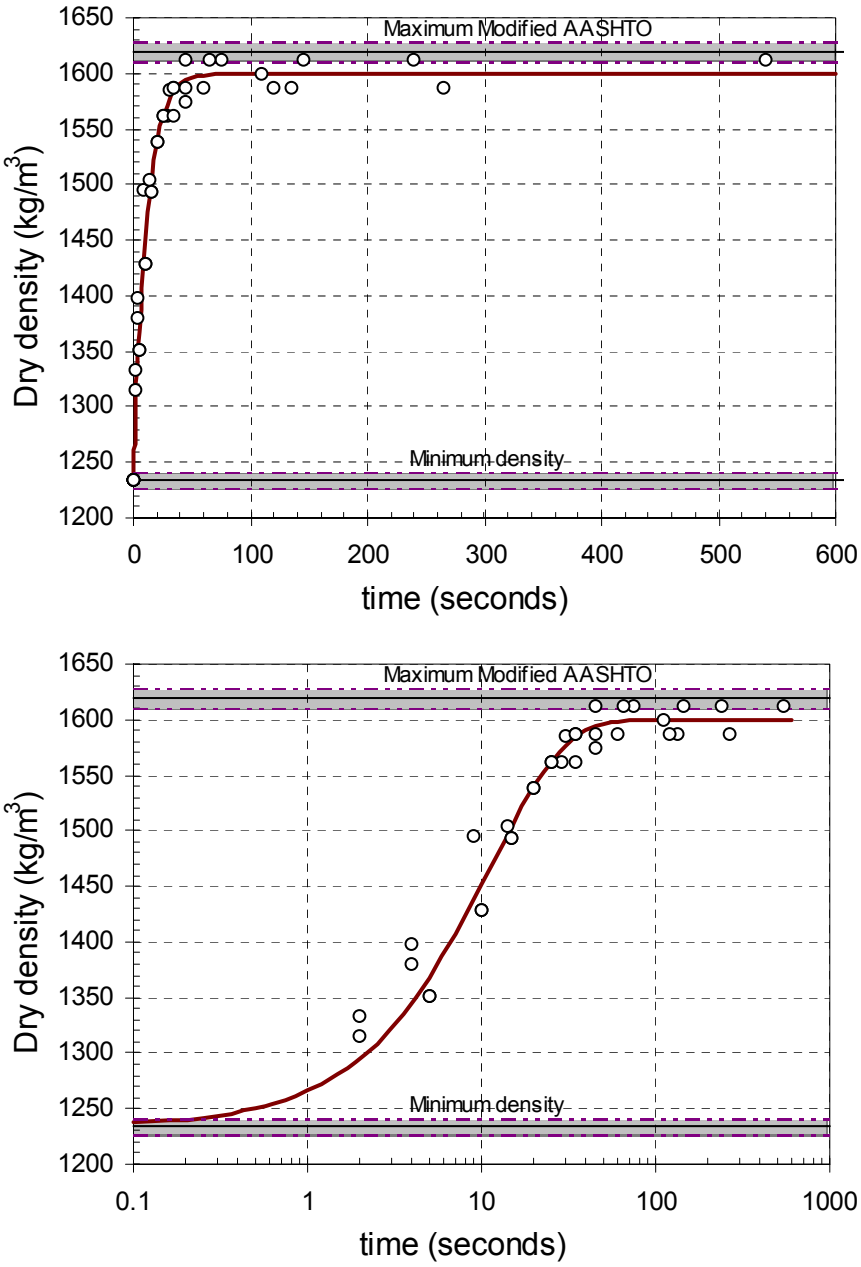

Figure 3.3 Results of the vibrating cylinder compaction test.

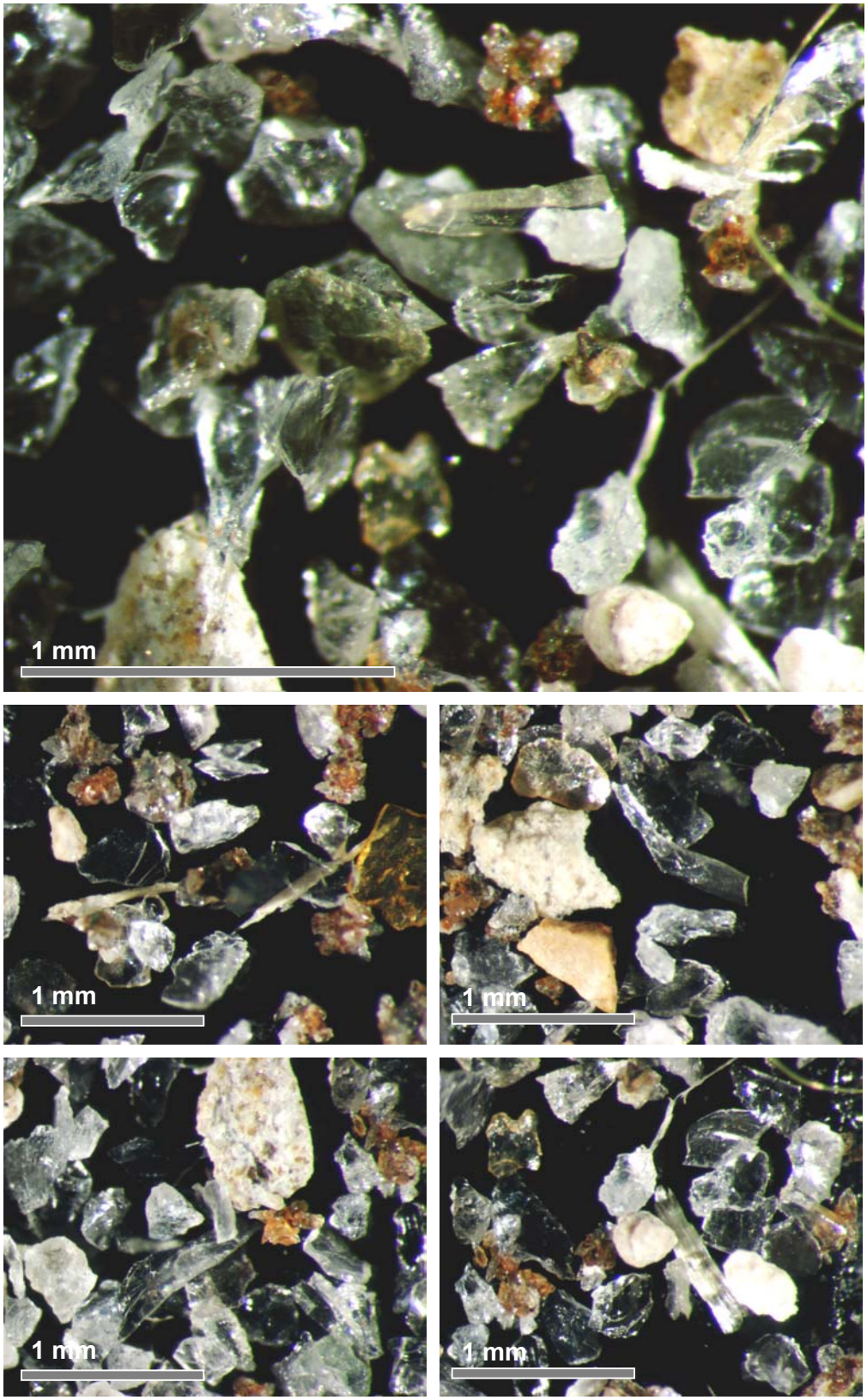

Figure 3.4 *Images from light microscopy on classified tailings retained on 212 μm sieve (scales approximate).*

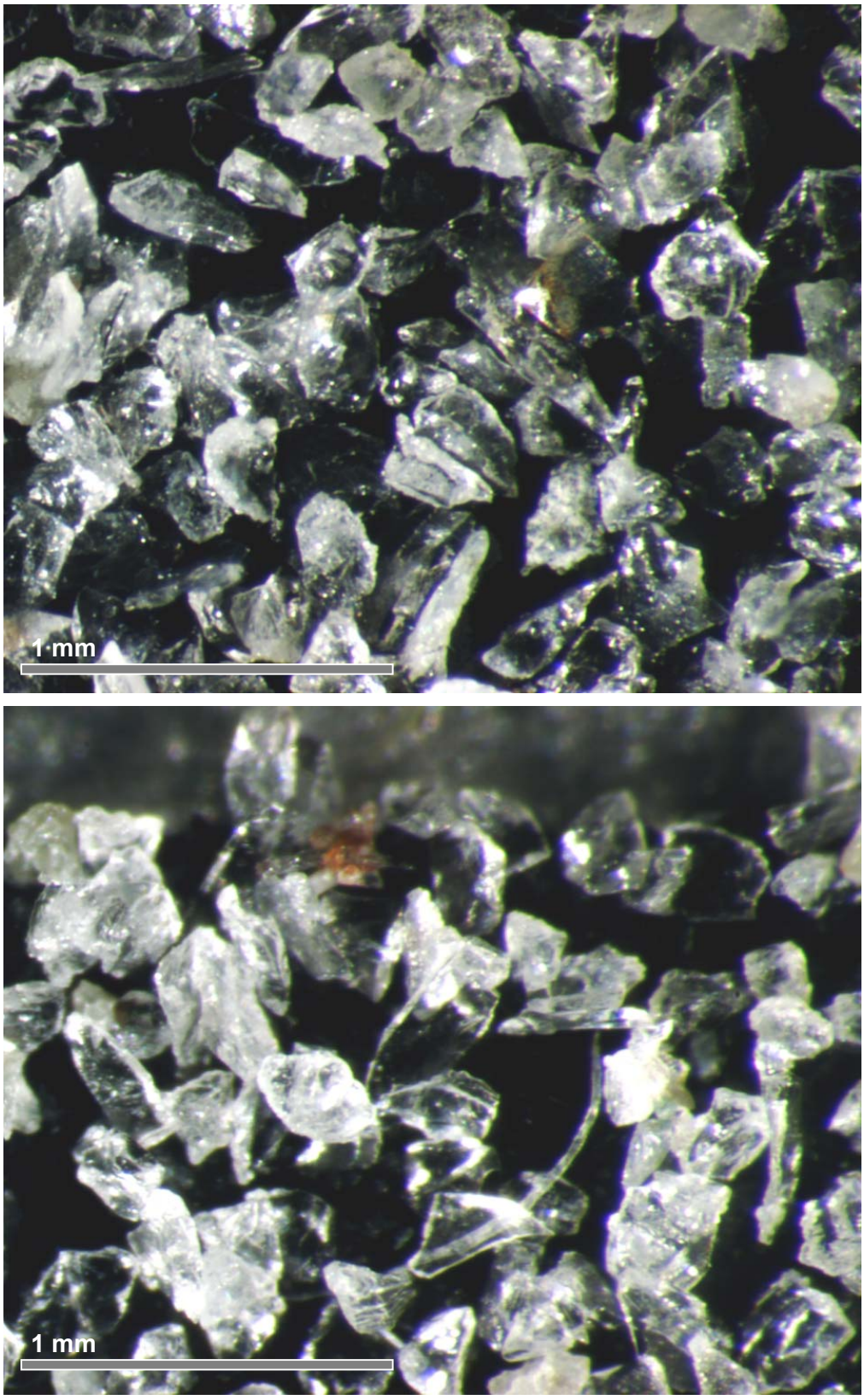

Figure 3.5 *Images from light microscopy on classified tailings retained on 150 μm sieve (scales approximate).*

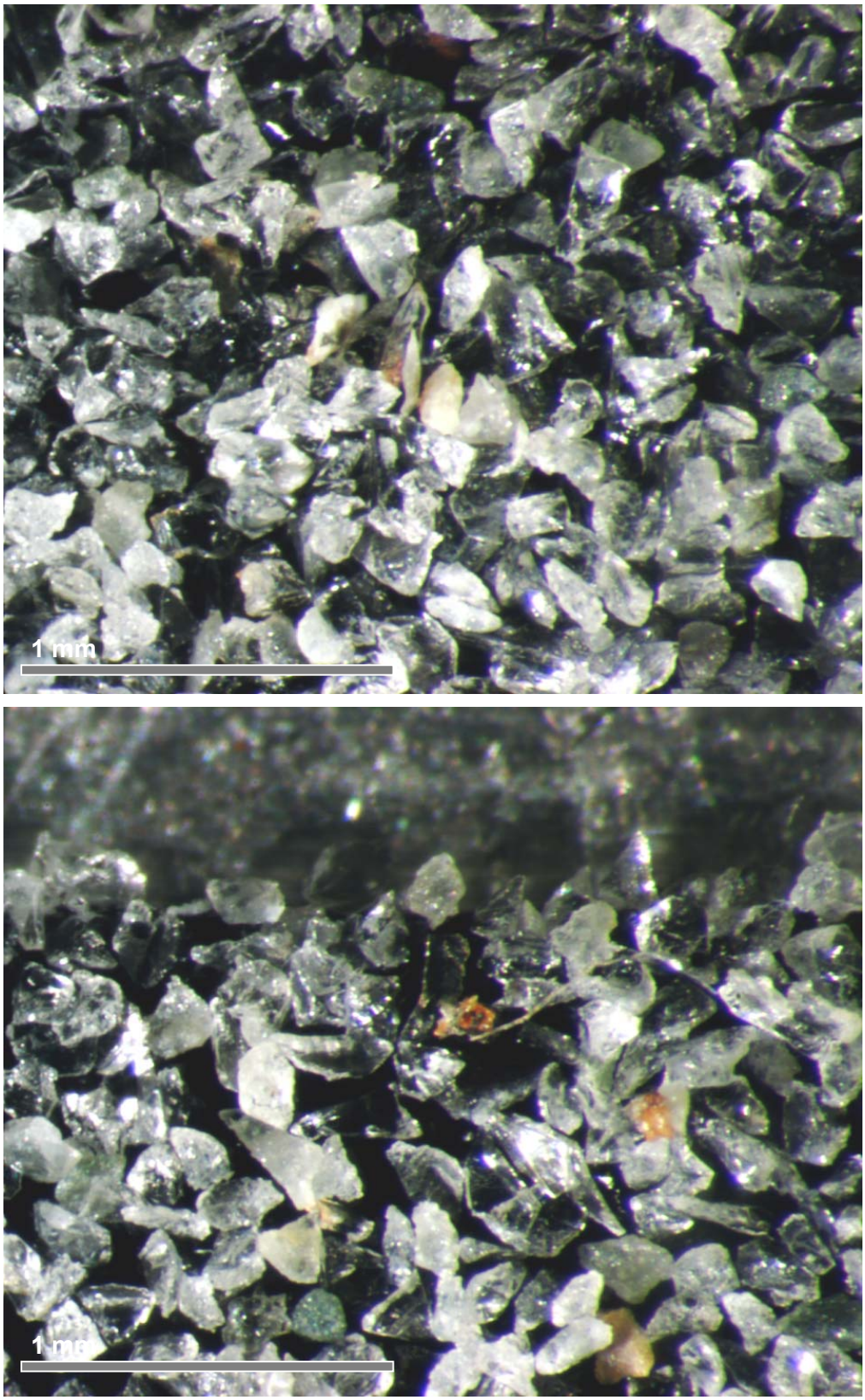

Figure 3.6 *Images from light microscopy on classified tailings retained on 125 μm sieve (scales approximate).*

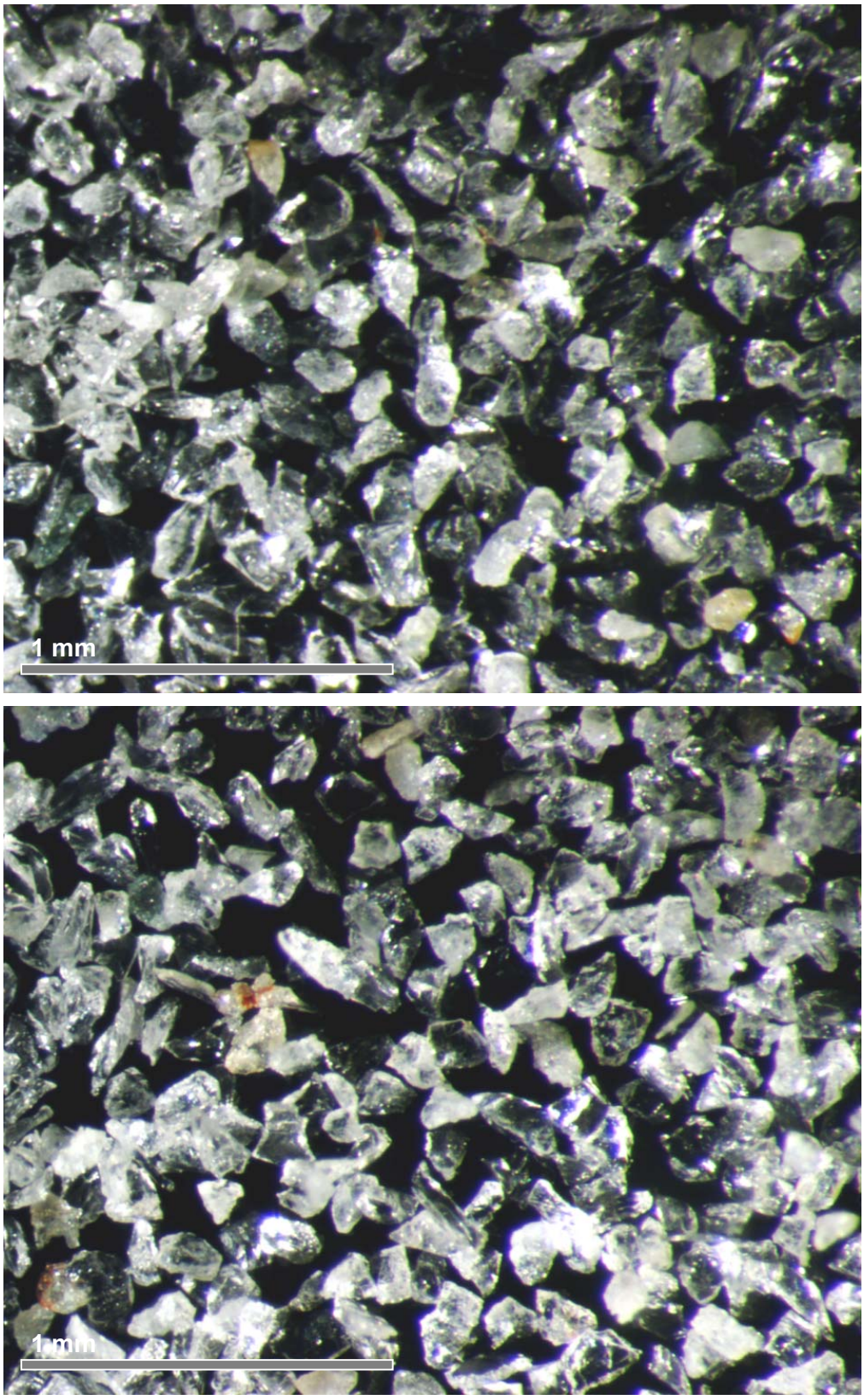

Figure 3.7 *Images from light microscopy on classified tailings retained on 75 μm sieve (scales approximate).*